

On the unique mapping relationship between initial and final quantum states

A. S. Sanz^{1,2*}, S. Miret-Artés¹

¹*Instituto de Física Fundamental (IFF-CSIC), Serrano 123, 28006 Madrid, Spain*

²*Department of Physics and Astronomy, University College London, Gower Street, London WC1E 6BT, United Kingdom*

Abstract

In its standard formulation, quantum mechanics presents a very serious inconvenience: given a quantum system, there is no possibility at all to unambiguously (causally) connect a particular feature of its final state with some specific section of its initial state. This constitutes a practical limitation, for example, in numerical analyses of quantum systems, which often make necessary the use of some extra assistance from classical methodologies. Here it is shown how the Bohmian formulation of quantum mechanics removes the ambiguity of quantum mechanics, providing a consistent and clear answer to such a question without abandoning the quantum framework. More specifically, this formulation allows to define probability tubes, along which the enclosed probability keeps constant in time all the way through as the system evolves in configuration space. These tubes have the interesting property that once their boundary is defined at a given time, they are uniquely defined at any time. As a consequence, it is possible to determine final restricted (or partial) probabilities directly from localized sets of (Bohmian) initial conditions on the system initial state. Here, these facts are illustrated by means of two simple yet physically insightful numerical examples: tunneling transmission and grating diffraction.

Keywords: Bohmian mechanics; quantum flux; quantum density current; probability tube; separatrix
PACS: 03.65.-w, 03.65.Ca, 03.65.Nk, 03.75.-b, 03.65.Xp

1. Introduction

Modern-day experimental techniques allow us to monitor the evolution of quantum systems in real time —e.g., the passage of electrons through barriers [1], the formation of diffraction patterns with complex molecules [2], or determining the (average) path followed by photons in Young’s two-slit experiment without destroying the interference pattern [3]. This possibility brings in a natural way the question of whether it would also be possible to establish an unambiguous connection between some particular feature of the final state of a quantum system and a specific subregion of its initial state. In principle, there are no means in our standard version of quantum mechanics to determine such an information in a unique way. Schrödinger’s equation describes how the whole quantum state of a system, specified by a wave function $\Psi(\mathbf{r}, t)$, evolves in time, but it is unable to provide an answer on how a particular piece of this wave function evolves or to see its effect on the final outcome.

In classical mechanics, such a question is not a problem at all. The connection can be established because, apart from statistical density distributions, one can also monitor the system along trajectories. The evolution of any phase space point (representing the system) can be monitored in time by means of a well-defined trajectory. These sets of trajectories, starting from a certain phase-space region Ω_0 , evolve

*Corresponding author
Email address: asanz@iff.csic.es (A. S. Sanz^{1,2})

according to a Liouvillian dynamics. There is a phase-space volume-preserving transformation that uniquely carries the initial conditions contained in Ω_0 onto a region Ω_t at a time t . That is, both regions are causally connected through a mapping or flow transformation $\Omega_t = \Phi(\Omega_0)$ [4–6]. In terms of statistical distributions, this translates into the continuity equation

$$\frac{\partial \rho}{\partial t} + \nabla \cdot \mathbf{J} = 0, \quad (1)$$

known in this context as the Liouville equation. In this equation, $\rho(\mathbf{x}, t)$ represents the probability distribution of trajectories in phase space (here $\mathbf{x} = (\mathbf{q}, \mathbf{p})$ denotes collectively the set of generalized positions and momenta defining this phase space) and a current density with the form $\mathbf{J}(\mathbf{x}, t) = \mathbf{F}(\mathbf{x})\rho(\mathbf{x}, t)$, where \mathbf{F} is defined in terms of the equation of motion describing the trajectories, $\dot{\mathbf{x}} = \mathbf{F}(\mathbf{x})$. This simple equation establishes the connection between the variation in time of the (trajectory) density distribution, ρ , contained in Ω_t at a time t and its flux or current density, \mathbf{J} , across the boundaries of Ω_t (henceforth, these boundaries will be denoted by $\partial\Sigma_t$). Although implicit in the quasi-classical trajectory method, this simple idea became the germ for a former methodological scheme aimed at determining reaction probabilities and product distributions by considering phase-space *reactivity bands* [7–9].

Here we show how to proceed in a similar fashion in quantum mechanics by making use of its Bohmian formulation. As it is shown, this hydrodynamical [10] or trajectory-based [11] formulation offers us a unique answer to the question posed above. Making use of the non-crossing property in configuration space of Bohmian trajectories [12, 13], we can define *probability tubes*, which are the quantum analog of the classical reactivity bands mentioned above. The interest of these particular tubes arises from the fact that, as far as we are concerned, Bohmian mechanics is the only formulation of quantum mechanics that allows to specify such elements in a unique way. Once the region Ω_0 is defined, one has a clear and unambiguous prescription to follow its causal evolution throughout configuration space. A mapping relation $\Omega_t = \Phi_Q(\Omega_0)$ (‘ Q ’ for ‘quantum map’) can also be used, given that Bohmian trajectories do not cross in configuration space and obey a continuity equation like (1) (with $\mathbf{x} = \mathbf{r}$). Thus, trajectories distributed along the boundary $\partial\Sigma_0$ of Ω_0 will subsequently form the boundary $\partial\Sigma_t$ of Ω_t . These are *separatrix trajectories* or, in short, *separatrices*. We would like to remark that, somehow, these properties have been empirically (numerically) observed in the analysis of single features in realistic simulations, for example, to determine the specific contribution of each part of the initial wave function to different diffraction features in realistic simulations of atom-surface interactions and lifetimes of selective adsorption resonances [14–17], to obtain estimates of product formation rates in model molecular systems [18, 19], or in the implementation of Monte-Carlo-Bohmian samplers employed in quantum initial value representation calculations [20–22]. Furthermore, the deformation of the tubes with time is not completely arbitrary, as it usually occurs in topology when dealing with deformations, since the non-crossing rule of trajectories has to be always preserved.

A direct consequence of dealing with quantum probability tubes is that, if we define a *partial* or *restricted probability* [18, 19, 23, 24] as the fraction of the total probability that has ended up inside a region or domain \mathcal{D} of the system configuration space,

$$\mathcal{P}_{\mathcal{D}}(\infty) \equiv \lim_{t \rightarrow \infty} \mathcal{P}_{\mathcal{D}}(t) = \lim_{t \rightarrow \infty} \int_{\mathcal{D}} \rho(\mathbf{r}, t) d\mathbf{r}, \quad (2)$$

it will remain constant in time whenever \mathcal{D} corresponds to a probability tube. This means that, in principle, asymptotic probabilities like (2) can be specified from the initial state without any further calculation if we know: (1) the analytical form for the separatrices defining the initial boundary $\partial\Sigma_0$, and (2) any *bifurcation* or *branching process* undergone by the probability tubes between t_0 and $t \rightarrow \infty$. The presence of branchings is actually a very important issue: any region Ω_t (including Ω_0) may consist of more than one separate subregions, which emerge or disappear along time.

This work has been organized as follows. The proof of the uniqueness of the probability tubes, as well as their definition and that of separatrix, are given in Sec. 2. The properties of these tubes are illustrated and analyzed in Sec. 3 in terms of two simple yet physically insightful one-dimensional numerical examples: tunneling transmission and grating diffraction (for more complex applications we refer the interested reader

to the references mentioned above). Finally, in Sec. 4 we summarize and discuss the main conclusions drawn from this work.

2. Theoretical background

Let $\mathcal{P}_{\Omega_t}(t)$ be a quantity describing the time-evolution of a certain probability of interest (e.g., a reaction probability, a transmittance, a cross-section, etc) inside a region Ω_t of the corresponding configuration space. This quantity is given in terms of the partial or restricted probability

$$\mathcal{P}_{\Omega_t}(t) \equiv \int_{\Omega_t} \rho(\mathbf{r}, t) d\mathbf{r}. \quad (3)$$

The variation of $\mathcal{P}_{\Omega_t}(t)$ with time inside Ω_t is

$$\frac{d\mathcal{P}_{\Omega_t}(t)}{dt} = \int_{\Omega_t} \frac{\partial \rho}{\partial t} d\mathbf{r}, \quad (4)$$

although it can also be written as

$$\frac{d\mathcal{P}_{\Omega_t}(t)}{dt} = - \int_{\Omega_t} (\nabla \cdot \mathbf{J}) d\mathbf{r} = - \int_{\partial\Sigma_t} \mathbf{J} \cdot d\mathbf{S}. \quad (5)$$

In the second equality of (5), which is a straightforward application of the divergence or Gauss-Ostrogradsky theorem, $d\mathbf{S}$ denotes a vector normal to a surface element $d(\partial\Sigma_t)$ of Ω_t and pointing outwards. By combining Eqs. (4) and (5), we find that the losses or gains of $\mathcal{P}_{\Omega_t}(t)$ inside Ω_t are described, respectively, by the outgoing or ingoing probability flux \mathbf{J} through $\partial\Sigma_t$. This is a well-known result, which translates into the continuity equation

$$\frac{\partial \rho}{\partial t} + \nabla \cdot (\mathbf{v}\rho) = 0. \quad (6)$$

when generalizing to the whole configuration space and making the flux to be independent of Ω_t . However, we obtain another interesting result if we still keep the dependence on Ω_t , for it also tells us that if the time-evolution of this region follows some particular rule, then one could keep the value of $\mathcal{P}_{\Omega_t}(t)$ constant all the way through.

The standard version of quantum mechanics does not give us any prescription to monitor in time portions of a given quantum system. Therefore, the choice of a time-evolution rule for Ω_t is left to arbitrariness. However, in the Bohmian formulation of quantum mechanics, the evolution of a system can be monitored by means of well-defined trajectories in configuration space. These trajectories are solutions to the equation of motion

$$\dot{\mathbf{r}} = \frac{\nabla S}{m} = \frac{\mathbf{J}}{\rho}. \quad (7)$$

where m is the mass associated with the system. In this equation, $S(\mathbf{r}, t)$ denotes the phase of the wave function when it is recast in polar form, i.e.,

$$\Psi(\mathbf{r}, t) = \rho^{1/2}(\mathbf{r}, t) e^{iS(\mathbf{r}, t)/\hbar}, \quad (8)$$

with $\rho = |\Psi|^2$ being the probability density, and $\mathbf{J}(\mathbf{r}, t)$ is the local quantum current density, defined as

$$\mathbf{J} = \frac{\hbar}{2mi} [\Psi^* \nabla \Psi - \Psi \nabla \Psi^*]. \quad (9)$$

As it can be noticed, Eq. (7) is identical to the classical Jacobi law of motion [25], although S is not the classical action—in semiclassical treatments, a relationship can be found between this quantum phase and the classical action [5]. In principle, Eq. (7) is postulated once the ansatz (8) is substituted into Schrödinger's

equation and two couple real equations arise, namely the continuity equation and the quantum Hamilton-Jacobi equation. However, such a reformulation will not be necessary here, since (7) can be introduced in a natural way as a local velocity field from the relation $\mathbf{J} = \rho\mathbf{v}$, directly connected with the continuity equation (6). Physically, this velocity field describes how the quantum probability density is transported through the configuration space in the form of the quantum probability current density. Notice that, according to Eq. (7), this field remains invariant if the wave function is multiplied by a time-dependent gauge factor $e^{ig(t)/\hbar}$, but not if such a gauge depends on the spatial coordinate, i.e., $e^{iG(x,t)/\hbar}$. In such a case, there will be a contribution $\nabla G(x,t)/m$ that will change locally (i.e., at each point x) the velocity field.

Now we already have all the elements to provide an answer to our question without abandoning the theoretical framework of quantum mechanics (notice that Bohmian mechanics constitutes another way to recast quantum mechanics, which must not be seen as a semiclassical-like approximation). Thus, consider that the boundary $\delta\Sigma_t$ consists of the positions $x(t)$ at t of a set of Bohmian trajectories. From the deterministic equation of motion (7) we can trace these trajectories back and also propagate them ahead in time. In any case, at any other time t' these trajectories will form another boundary $\delta\Sigma_{t'}$. Moreover, as happens with their classical counterparts in phase space, which cannot cross through the same point at the same time, Bohmian trajectories are also constrained to move in configuration space without crossing [12, 13]. Accordingly, the arbitrariness of quantum mechanics is thus removed, since we now have a clear and unambiguous prescription to follow the evolution of a certain region Ω_t in time.

The trajectories forming the boundary $\delta\Sigma_t$ play the role of separatrices, since trajectories outside Ω_t cannot penetrate this region, nor those inside can leave it. This means that the probability inside Ω_t remains always constant in time. Hence, we can define quantum probability tubes as the structures formed by the time-evolution of Ω_t . If the dimensionality of the problem is N (N is the number of degrees of freedom), these tubes will have a $(N + 1)$ -dimensionality. These tubes are uniquely selected once a specific region of the configuration space has been chosen. For example, in a scattering problem, if we define a number M of regions $\Omega_t^{(m)}$ ($m = 1, 2, \dots, M$), each one covering one particular diffraction feature, when we trace them back in time, we will obtain a full map of regions $\Omega_0^{(m)}$ covering the initial wave function and providing us information about the sets of initial conditions that have given rise to such diffraction features (see, for example, Ref. [14]).

From the above statements we obtain an interesting consequence: any restricted probability can be determined directly from the initial state if the end points of the associated separatrix trajectories as well as any intermediate branching process are known. That is, in principle one could determine (or, at least, get an estimate of) final probabilities without carrying out the full calculation, but directly from the particular region covered by the initial wave function causally connected with the feature of interest [26]. The proof is very simple and follows straightforwardly from the possibility to define probability tubes. Consider that in the restricted probability (2), the domain \mathcal{D} corresponds to the region Ω_∞ , which is the asymptotic extreme of a probability tube starting in Ω_0 at $t = 0$. By integrating back in time (i.e., considering the inverse mapping transformation $\Omega_0 = \Phi_Q^{-1}(\Omega_\infty)$), we find

$$\mathcal{P}_{\Omega_\infty} = \int_{\Omega_\infty} \rho(\mathbf{r}, \infty) d\mathbf{r} = \lim_{t \rightarrow \infty} \int_{\Omega_t} \rho(\mathbf{r}, t) d\mathbf{r} = \lim_{t \rightarrow \infty} \mathcal{P}_{\Omega_t}(t). \quad (10)$$

The difference of this expression with respect to Eq. (7) is that now we can keep track of the amount of probability going into $\mathcal{D} = \Omega_\infty$ by means of an unambiguous time-dependent relationship. But, since the probability inside the corresponding tube remains constant, we can just write down (10) as

$$\mathcal{P}_{\Omega_\infty} = \int_{\Omega_0} \rho(\mathbf{r}, 0) d\mathbf{r} = \mathcal{P}_{\Omega_0}(0). \quad (11)$$

The initial restricted probability \mathcal{P}_{Ω_0} can be computed from an appropriate sampling of (Bohmian) initial conditions (according to $\rho(\mathbf{r}, 0)$) inside Ω_0 , as in classical mechanics. By proceeding in this way, the physical meaning of Eq. (11) becomes more apparent (and almost trivial): given a certain set of initial conditions enclosed in some region of the configuration space, their total number is conserved regardless of how the

ensemble evolves. This is a result of *general* validity, which goes again beyond standard quantum mechanics, for it states that the probability within a certain region of the configuration space can be transported to another one causally connected, i.e., in an unambiguous fashion when following probability tubes.

3. Numerical simulations

3.1. Tunneling

To test the feasibility of the concepts exposed in Sec. 2 and, in particular, the applicability of Eq. (11) regardless of the initial state or the problem considered, consider the scattering of a wave function off a barrier. This tunneling problem may describe, for example, the passage from reactants to products in a chemical reaction. Thus, let us consider as the initial wave function an arbitrary coherent superposition of three Gaussian wave packets,

$$\Psi_0(x) = A_0 \sum_{i=1}^3 c_i \psi_i(x), \quad (12)$$

where each ψ_i is described by

$$\psi_0(x) = \left(\frac{1}{2\pi\sigma_0^2} \right)^{-1/4} e^{-(x-x_0)^2/4\sigma_0^2 + ip_0(x-x_0)/\hbar}, \quad (13)$$

with x_0 and p_0 being respectively the (initial) position and momentum of the wave-packet centroid (i.e., $\langle \hat{x} \rangle = x_0$ and $\langle \hat{p} \rangle = p_0$), and σ_0 its initial spreading. Without loss of generality, the parameters chosen are: $(c_1, c_2, c_3) = (1.0, 0.75, 0.5)$, $(x_{0,1}, x_{0,2}, x_{0,3}) = (-10, -12, -9)$, $(p_{0,1}, p_{0,2}, p_{0,3}) = (10, 20, 15)$, $(\sigma_{0,1}, \sigma_{0,2}, \sigma_{0,3}) = (0.2, 1.6, 0.8)$, and $m = \hbar = 1$; after introducing these values, the wave function Ψ_0 is properly renormalized before starting the simulation, this being denoted by the constant prefactor A_0 in (12). As for the barrier, we take a nearly square barrier consisting of a sum of two hyperbolic tangents,

$$V(x) = \frac{V_0}{2} \{ \tanh[\alpha(x - x_-)] - \tanh[\alpha(x - x_+)] \}, \quad (14)$$

with $V_0 = 150$, $\alpha = 10$, and $x_{\pm} = \pm 2$. The simulation was carried out by means of a standard wave-packet propagation method [27–29], while the associated Bohmian trajectories were computed “on-the-fly”, substituting the wave function resulting at each iteration into (7) and then integrating this equation of motion.

The initial and final probability densities are displayed in Fig. 1(a) (black and red solid lines, respectively); the barrier has also been plotted (blue shadowed region). The system wave function was evolved until the probability within the intra-barrier region was negligible, this being assumed to be our asymptotic time. This can be better seen in panel (b), where the transmission (green dashed line), reflection (blue dash-dotted line) and intra-barrier (red dotted line) probabilities are monitored along time. In the calculation of these restricted probabilities it was assumed that: \mathcal{D}_T is the region beyond the right-most barrier edge, \mathcal{D}_I is the region confined between the two barrier edges, and \mathcal{D}_R is the region to the left-most edge. As seen in the figure, after $t \approx 1.15$, we find that $\mathcal{P}_R \approx 0$ and \mathcal{P}_T reaches its maximum (asymptotic) value, which already remains constant with time.

Let us split up the initial wave function into “reflectable” and “transmittable”, with Ω_0 encompassing the portion associated with the latter. The upper bound for this region can be the initial position, $x(0)$, of any trajectory on the right-most border of the initial probability density, for which $\rho(x(0)) \approx 0$. For the lower boundary, a search has to be done [26], so that it is ensured that the chosen trajectory is the last (or nearly the last) one in crossing the right-most barrier edge and not displaying a backwards motion. Determining this trajectory constitutes a major drawback, since Bohmian trajectories are not analytical in general, neither there is a simple, general way to make an estimate [26]. This initial condition has to be then determined either from a series of sampling runs or just fixing the asymptotic value of the trajectory and running backwards in time the dynamics until $t = 0$.

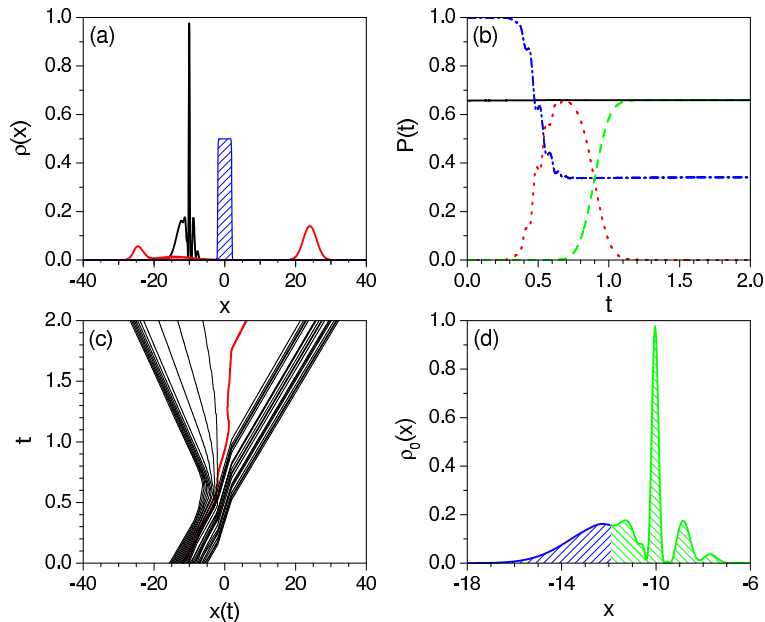


Figure 1: (a) Initial (black line) and final (red line) probability densities in the problem of scattering off a nearly square barrier (blue shadowed region). (b) Time-dependence of the transmission (green dashed line), reflection (blue dash-dotted line) and intra-barrier (red dotted line) probabilities. The probability enclosed in Ω_t and obtained with the aid of the Bohmian calculation is displayed with black solid line. (c) Bohmian trajectories illustrating the process dynamics; the separatrix is denoted with red thicker line. (d) Splitting of the initial probability density according to the separatrix initial position. Only the green shadowed region (Ω_0) contributes to transmission.

A sampling set of Bohmian trajectories is shown in Fig. 1(c), with their initial positions evenly distributed along the extension covered by the initial probability density. The red thicker line denotes the separatrix splitting the initial swarm into two groups of trajectories: those that will surmount the barrier (transmitted) and those that will bounce backwards (reflected). Accordingly, at any time t , the region Ω_t (i.e., the time-evolved of Ω_0) always confines trajectories that eventually become transmitted; $\partial\Sigma_t$ is determined by the positions at t of two trajectories, namely the separatrix and the rightmost one considered. The evolution of these two trajectories defines the corresponding transmission probability tube, along which all the transmitted probability density flows.

Bearing this scheme in mind, it is now rather simple and straightforward to determine which part of the initial probability density contributes to tunneling transmission, denoted by the green shadowed area in panel (d). The integral over this area readily provides the value otherwise found from the asymptotic \mathcal{P}_T (see panel (b)). Actually, the evaluation of $\mathcal{P}_{\Omega_t}(t)$ at each time renders a constant value (see black solid line in panel (b)), thus proving the conservation of the probability inside Ω_t . Furthermore, this also proves our assertion that final probabilities can be, in principle, directly and unambiguously obtained from the initial state by means of Bohmian trajectories.

3.2. Grating diffraction

Consider now that we would like to determine, for example, the so-called *peak-intensity area* in a scattering problem, i.e., the total intensity that goes into a certain diffraction peak or, equivalently, the relative amount of scattered particles lying within the area covered by this diffraction peak. This value is obtained by computing the integral of the probability density lying between the two adjacent minima associated with such a diffraction peak. One could be legitimated to ask about which parts of the diffracted beam contribute to a particular diffraction peak, or how each particular feature of the diffracting object contributes to a final diffraction feature. These questions cannot be answered within the standard version of quantum mechanics.

However, the tools so far developed can be used to provide reasonable answers (i.e., coherent with the use of a full quantum framework), in particular Eq. (11).

To illustrate this situation, we are going to analyze five-slit diffraction [15], which is also a good example to observe branching processes and bifurcations of the probability tubes. We shall consider our initial wave function to be the diffracted beam. Let us then assume that spatial variations along the direction perpendicular to the grating are negligible compared to the transversal ones and the propagation (along that direction) is faster. This working hypothesis allows us to characterize the process by a wave function that only accounts for what happens in the transversal direction. If we also assume slit Gaussian transmission, the initial wave function can be expressed as a coherent superposition of five Gaussian wave packets,

$$\Psi_0(x) = A_0 \sum_{i=1}^5 \psi(x), \quad (15)$$

where each wave packet is given by (13), with $x_0^{(i)} = -4 + 2(i-1)$, $p_0^{(i)} = p_0 = 0$ (zero transverse momentum), $\sigma_0^{(i)} = \sigma_0 = 0.2$, and $m = \hbar = 1$; as before, A_0 is the renormalization constant. Regarding the numerical simulation, we have followed the same procedure as in Sec. 3.1. Propagation up to $t = 10$ produces diffraction peaks that are already well resolved, but with nonzero adjacent minima, as seen in Fig. 2(a). This can be the case, for example, when the detector is allocated relatively close to the grating, so that the system has not been able yet to reach the Fraunhofer regime [14]. The corresponding Bohmian dynamics is illustrated with the trajectories displayed in panel (b), with initial conditions evenly distributed along the effective extension covered by each wave packet.

Consider the principal maxima associated with the diffraction orders $n = 0$ and $n = +1$ in panel (a). Let $\Omega_0 \equiv \{x_0^-, x_0^+\}$ and $\Omega_{+1} \equiv \{x_{+1}^-, x_{+1}^+\}$ be the sections of the initial wave function, such that at $t = 10$ cover the principal maxima $n = 0$ and $n = +1$, respectively, between their corresponding adjacent minima (see color shaded regions in the figure). The restricted probabilities associated with these two regions give us the value of the respective peak-intensity areas. From a standard quantum viewpoint, one could be tempted to define some associated sectors or domains, \mathcal{D}_n , taking into account the Fraunhofer limit, where minima vanish. More specifically, the domain \mathcal{D}_n for the n th diffraction peak would cover the extension between the corresponding adjacent minima. According to the Fraunhofer diffraction formula for this case [30], the boundaries for \mathcal{D}_n evolve with time¹ as

$$x_n^\pm(t) = 2\pi(N \pm 1) \left(\frac{n}{N}\right) \left(\frac{\hbar}{md}\right) t, \quad (16)$$

with $N = 5$ and $d = 2$, and where $+/-$ refers to the right/left boundary. Notice that this expression is valid within the Fraunhofer regime, where minima vanish; for shorter times, these boundaries will pass through positions with nonzero probability density and, at $t = 0$, all boundaries will coalesce on $x = 0$. In panel (b) the boundaries for the diffraction orders $n = 0$ and $n = +1$ are shown (straight trajectories of the same color as the corresponding shaded areas from panel (a)).

From a practical viewpoint, computing restricted probabilities with the aid of these domains \mathcal{D}_n thus requires to be in the Fraunhofer regime, which is troublesome in the sense that this condition is not always fulfilled. This is precisely what we observe in panel (c), where the restricted probabilities within the domains \mathcal{D}_0 (blue dashed line) and \mathcal{D}_{+1} (red dotted line) have been computed. Asymptotically, they approach a constant value, which has been obtained by means of proper Bohmian boundaries (see below). Thus, at $t = 20$ the deviations with respect to these asymptotic values are relatively small (about 1.72% for $n = 0$ and 1.68% for $n = +1$). However, for smaller values of time, discrepancies become more relevant. The problem with these domains is that there is no way to determine the origin of these divergences (other than the lack of validity of expression (16)) and therefore to control them.

¹It does not make any sense to consider in this case of fixed domain, because the wave function is spreading all the way through —even in the Fraunhofer regime, where this spreading is linear with time, although the relative shape remains invariant.

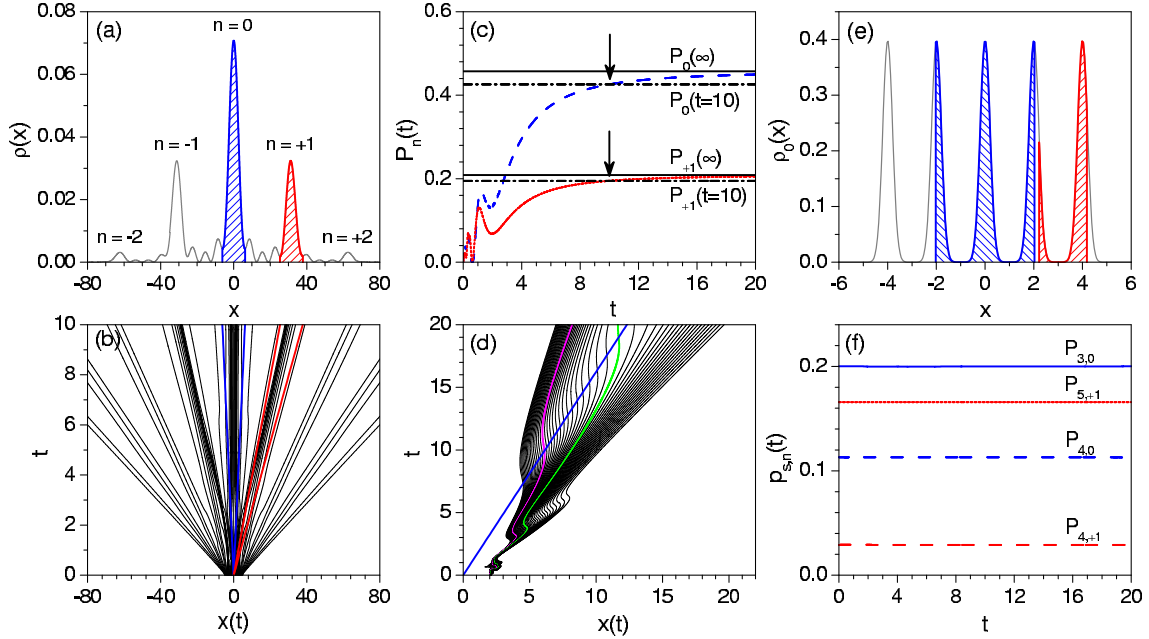


Figure 2: (a) Five-slit diffraction pattern at $t = 10$. Principal maxima are labeled according to their diffraction order, n ; shaded color areas denote the computed peak-intensity areas. (b) Bohmian trajectories illustrating the diffraction dynamics. The domains \mathcal{D}_0 and \mathcal{D}_{+1} for the maxima highlighted in (a) are enclosed by the boundaries x_0^\pm (blue) and x_{+1}^\pm (red), respectively (see text for details). (c) Peak-intensity areas corresponding to the diffraction orders $n = 0$ (blue dashed line) and $n = +1$ (red dotted line). The peak-intensity areas directly computed from the initial state are denoted with black solid line for $t = 20$ (asymptotic time) and black dash-dotted line for $t = 10$. (d) Set of Bohmian trajectories around the separatrix for the peak $n = 0$ at $t = 10$ (purple thicker line). The separatrix at $t = 20$ and the boundary x_0^+ (see text for details) are represented with green and blue thicker lines, respectively. (e) Sections of the initial probability density that give rise to the $n = 0$ (blue shaded section) and $n = +1$ (red shaded section) diffraction peaks at $t = 10$ (see panel (a)). (f) Contributions from slits 3, 4 and 5 to the $n = 0$ and $n = +1$ diffraction peaks (see panel (d)).

To understand such a behavior, we need to consider Bohmian trajectories and have a look at their topology. In panel (d) we show a swarm of trajectories with very close and evenly distributed initial conditions (they cover 0.030 space units). As seen, these trajectories start on the right side of x_0^+ ; as time proceeds, some of them start crossing this boundary; eventually, they split into two groups, each one contributing to a different diffraction peak, namely $n = 0$ and $n = +1$, in spite of their initial proximity. This is a clear example of branching processes, as mentioned in Sec. 2. In these cases where we are not yet in the Fraunhofer domain, it is thus important to make clear what the asymptotic time is, since the separatrix at one time can be useless at another time. For example, at $t = 0$ the separatrix is denoted by the purple thicker line in panel (d), which renders restricted probabilities for $n = 0$ and $n = +1$ about 6.92% and 6.70% lower than the corresponding asymptotic ones (see black solid lines in panel (c)). This means that about 6.92% and 6.70% of trajectories are still lacking in the calculation of the corresponding peak areas, as it is inferred by looking at the separatrix denoted with the green thicker line in panel (d).

Finally, given the presence of branching, one may be interested in determining how much each slit contributes to the final pattern, also from the initial state. This can be easily done with the aid of the separatrix trajectories, which allow us to establish which is the range of the initial wave function contributing to each diffraction peak and therefore the source slit. Thus, in panel (e) we observe that the whole central slit and more than a half of the adjacent ones contribute to the $n = 0$ diffraction peak (see blue shadowed areas), while a small portion of the third slit and a large one of the fifth slit contribute to $n = +1$ (see red shadowed areas). By integrating these portions of initial wave function, we can now provide a quantitative measure of the relative contribution of each slit, as shown in panel (f). In this figure, $\mathcal{P}_{i,n}$ refers to the

restricted probability contributing to the n th diffraction peak and coming from the i th slit.

4. Concluding remarks

We have shown how final features of quantum probabilities can be unambiguously related to different sections of the initial state by using Bohmian mechanics. This fact certainly reminds of some classical statistical approaches that can be found in different fields, e.g., chemical reactivity [7–9] or atmospheric modeling [31, 32]. More specifically, such a connection is enabled through the combination of the divergence or Gauss-Ostrogradsky theorem with Bohmian mechanics, which allows to go a step beyond the standard formulation of quantum mechanics and to devise new tools to study and to understand the physics underlying of quantum systems. In particular, even if not observable from a experimental point of view, the fact that one can properly define (in terms of separatrices) regions that are uniquely transported throughout the system configuration space without loss or gain of quantum flux results of much interest to study the dynamical role of quantum phase in time-resolved experiments. Note that this methodological prescription allows to monitor the detailed evolution of a set of particular initial conditions and, therefore, to determine the final outcome (probability) directly from the initial state. In this sense, it can be considered as an extension to time-dependence of Born’s rule (see Appendix below). Actually, even if one does not know where such a particular set or part of the initial wave function will evolve, it is sure that the probability confined within its boundaries (separatrices) will not mix up with contributions from other parts of the same initial wave function. Within the standard scenario, however, there is no certainty about this and hence one has to appeal to rather arbitrary (classical or semiclassical) methods and/or arguments to determine final restricted probabilities.

A criticism that could be risen against this approach, though, is that the Bohmian probability tubes depend on the initial wave function (they are *context dependent*) and therefore varying the latter unavoidably leads to a change of the topology of the tubes (even for the same physical problem). For example, consider the case of tunneling analyzed above. Once the transmitted part is known, one can determine the region of the initial state that gives rise to such a transmission. However, the same tube cannot be used to analyze a new initial wave function. More specifically, in the context of concrete computations, the choice of the initial wave function will conform with some physical limitations, e.g., it is meaningless to consider an initial wave function not localized around the domain of initial conditions whose transmission is studied. Now, since the topology displayed by Bohmian trajectories is sensitive to the particular form adopted by the initial wave function, it is clear that such limitations are also going to restrict the relevance of contextual issues from a practical (computational) viewpoint. That is, by limiting the number of possible initial states, feasible boundaries for the corresponding probability tubes are also being somehow determined. Therefore, even if the true boundary is not known with a high accuracy, at least one has a fair estimate of it, which can be used for practical purposes [26]. Nonetheless, in any case, it is important to stress that this contextual dependence is not a problem of the approach itself (nor of Bohmian mechanics, generally speaking), but a property of quantum mechanics, which manifests more remarkably through Bohmian mechanics. Any quantum outcome is thus strongly dependent on the initial ensemble considered (i.e., the whole wave function), contrary to what we find in classical mechanics when considering trajectories in phase space, where the particle distribution does not influence the final outcome (and therefore the definition of classical tubes). This context-dependence appears, for example, in quantum control schemes [33], which are based on this property: by manipulating the initial state in a particular way, we can inhibit or enhance a certain final property.

There is another important issue worth stressing, which could also be considered as a drawback. It arises when dealing with chaotic and/or large systems, and is common to any trajectory-based methodology, including classical ones. In such cases, one only knows where the trajectories go after completion of the simulation. Thus information about the system dynamics is always extracted a posteriori, which is useful, though, to interpret reaction probabilities or momentum/energy transfers solely. In such cases, notice that multi-dimensional tubes with multiple branches may appear, thus making relatively complex the analysis of the system under study. Even though, such an analysis is still possible and useful, because it allows us to classify sets of initial conditions according to the type of dynamics that they will lead to.

The approach posed here, in principle, could be used to compute probabilities without any need for solving the full dynamics of the process, but only with some knowledge provided by the quantum trajectories. In practice, due to the non-analyticity of Bohmian trajectories, this cannot be easily done. However, it should be mentioned that in the literature somehow related methods can be found, which operate the other way around, i.e., from probability densities they try to infer the corresponding quantum trajectories without solving the associated equations of motion. This is the case, for example, of the Bohmian Monte Carlo sampling method [34], based on the idea of quantile motion [35], or the kinematic approach [36], based on Voronoi's tessellations method [37].

Acknowledgements

Support from the Ministerio de Economía y Competitividad (Spain) under Projects and FIS2010-22082 and FIS2011-29596-C02-01, as well as from the COST Action MP1006 (*Fundamental Problems in Quantum Physics*) is acknowledged. The authors are grateful to anonymous referees for useful comments. A. S. Sanz thanks the Ministerio de Economía y Competitividad for a “Ramón y Cajal” Research Fellowship and the University College London for its kind hospitality.

Appendix. Bohm-Born rule

The results discussed in Sec. 2 lead us straightforwardly to establish a connection with the so-called Born rule [38–41]. Actually, the aforementioned combination of the quantum continuity equation and Bohmian mechanics makes Eq. (11) to implicitly contain a kind of time-dependent Born rule. This is readily seen as follows. Consider two arbitrary times, t and t' (we will assume $t' > t$). It follows from Eq. (11) that

$$\int_{\mathbf{r}(t')} \rho[\mathbf{r}(t')] d\mathbf{r}(t') = \int_{\mathbf{r}(t)} \rho[\mathbf{r}(t)] d\mathbf{r}(t). \quad (\text{A.1})$$

On the other hand, because of the causal connection between $\mathbf{r}(t)$ and $\mathbf{r}(t')$ in Bohmian mechanics, one can also define a Jacobian

$$\mathcal{J}[\mathbf{r}(t)] = \frac{\partial \mathbf{r}(t')}{\partial \mathbf{r}(t)}, \quad (\text{A.2})$$

which describes the mapping transformation in configuration space from $x(t)$ at a time t to $x(t')$ at a time t' . This relation is equivalent to the one found in classical mechanics when solving the (classical) continuity equation [4–6], although in that case it includes the corresponding momenta, since it is defined in phase space. Thus, taking into account the equality (A.1) and the connection between the layers defined by $d\mathbf{r}(t)$ and $d\mathbf{r}(t')$ enabled by the Jacobian,

$$d\mathbf{r}(t') = |\mathcal{J}[\mathbf{r}(t)]| d\mathbf{r}(t), \quad (\text{A.3})$$

the probability density evaluated along a quantum trajectory at a time t' is related through the inverse Jacobian transformation with its value at an earlier time t , as

$$\rho[\mathbf{r}(t')] = |\mathcal{J}[\mathbf{r}(t)]|^{-1} \rho[\mathbf{r}(t)], \quad (\text{A.4})$$

with $|\mathcal{J}[\mathbf{r}(t')]| = |\mathcal{J}[\mathbf{r}(t)]|^{-1}$. That is, Born's rule is preserved along time whenever the evolution of the probability $\rho[\mathbf{r}(t)]$ is monitored within the probability tube defined by the swarms of quantum trajectories $\mathbf{r}(t)$ and $\mathbf{r}'(t) = [\mathbf{r} + d\mathbf{r}](t)$:

$$\rho[\mathbf{r}(t')] d\mathbf{r}(t') = \rho[\mathbf{r}(t)] d\mathbf{r}(t). \quad (\text{A.5})$$

References

- [1] M. Uiberacker, T. Uphues, M. Schultze, A. J. Verhoef, V. Yakovlev, M. F. Kling, J. Rauschenberger, N. M. Kabachnik, H. Schröder, M. Lezius, K. L. Kompa, H.-G. Müller, M. J. J. Vrakking, S. Hendel, U. Kleineberg, U. Heinzmann, M. Drescher, F. Krausz, Attosecond real-time observation of electron tunneling in atoms, *Nature* 446 (2007) 627–632.
- [2] S. Gerlich, S. Eibenberger, M. Tomandl, S. Nimmrichter, K. Hornberger, P. J. Fagan, J. Tüxen, M. Mayor, M. Arndt, Quantum interference of large organic molecules, *Nat. Commun.* 2 (2011) 263(1–5).
- [3] S. Kocsis, B. Braverman, S. Ravets, M. J. Stevens, R. P. Mirin, L. K. Shalm, A. M. Steinberg, Observing the average trajectories of single photons in a two-slit interferometer, *Science* 332 (2011) 1170–1173.
- [4] M. C. Gutzwiller, *Chaos in Classical and Quantum Mechanics*, Springer-Verlag, New York, 1990.
- [5] R. Guantes, A. S. Sanz, J. Margalef-Roig, S. Miret-Artés, Atom-surface diffraction: a trajectory description, *Surf. Sci. Rep.* 53 (2004) 199–330.
- [6] A. S. Sanz, S. Miret-Artés, Selective adsorption resonances: Quantum and stochastic approaches, *Phys. Rep.* 451 (2007) 37–154.
- [7] E. Pollak, M. S. Child, Classical mechanics of a collinear exchange reaction: A direct evaluation of the reaction probability and product distribution, *J. Chem. Phys.* 73 (1980) 4373–4380.
- [8] E. Pollak, Classical analysis of collinear light atom transfer reactions, *J. Chem. Phys.* 78 (1983) 1228–1236.
- [9] D. J. Tannor, *Introduction to Quantum Mechanics: A Time-Dependent Perspective*, University Science Books, Sausalito, CA, 2006.
- [10] E. Madelung, Quantentheorie in hydrodynamischer Form, *Z. Phys.* 40 (1926) 322–326.
- [11] D. Bohm, A suggested interpretation of the quantum theory in terms of “hidden” variables. I, *Phys. Rev.* 85 (1952) 166–179.
- [12] A. S. Sanz, S. Miret-Artés, A trajectory-based understanding of quantum interference, *J. Phys. A: Math. Theor.* 41 (2008) 435303(1–23).
- [13] A. S. Sanz, S. Miret-Artés, *A Trajectory Description of Quantum Processes. I. Fundamentals*, Springer, Berlin, 2012.
- [14] A. S. Sanz, F. Borondo, S. Miret-Artés, Causal trajectories description of atom diffraction by surfaces, *Phys. Rev. B* 61 (2000) 7743–7751.
- [15] A. S. Sanz, F. Borondo, S. Miret-Artés, Particle diffraction studied using quantum trajectories, *J. Phys.: Condens. Matter* 14 (2002) 6109–6145.
- [16] A. S. Sanz, F. Borondo, S. Miret-Artés, Quantum trajectories in atom-surface scattering with single adsorbates: The role of quantum vortices, *J. Chem. Phys.* 120 (2004) 8794–8806.
- [17] A. S. Sanz, F. Borondo, S. Miret-Artés, Role of quantum vortices in atomic scattering from single adsorbates, *Phys. Rev. B* 69 (2004) 115413(1–5).
- [18] A. S. Sanz, X. Giménez, J. M. Bofill, S. Miret-Artés, Understanding chemical reactions within a generalized Hamilton-Jacobi framework, *Chem. Phys. Lett.* 478 (2009) 89–96.
- [19] A. S. Sanz, X. Giménez, J. M. Bofill, S. Miret-Artés, Erratum to ‘Understanding chemical reactions within a generalized Hamilton-Jacobi framework’ [*Chem. Phys. Lett.* 478 (2009) 89], *Chem. Phys. Lett.* 488 (2010) 235–236.
- [20] E. R. Bittner, Quantum initial value representation using approximate Bohmian trajectories, *J. Chem. Phys.* 119 (2003) 1358–1364.
- [21] Y. Zhao, N. Makri, Bohmian versus semiclassical description of interference phenomena, *J. Chem. Phys.* 119 (2003) 60–67.
- [22] J. Liu, N. Makri, Monte Carlo Bohmian dynamics from trajectory stability properties, *J. Phys. Chem. A* 108 (2004) 5408–5416.
- [23] A. S. Sanz, S. Miret-Artés, Quantum trajectories in elastic atom-surface scattering: Threshold and selective adsorption resonances, *J. Chem. Phys.* 122 (2005) 014702(1–12).
- [24] A. S. Sanz, D. López-Durán, T. González-Lezana, Investigating transition state resonances in the time domain by means of Bohmian mechanics: The F+HD reaction, *Chem. Phys.* 399 (2012) 151–161.
- [25] H. Goldstein, C. Poole, J. Safko, *Classical Mechanics*, Addison Wesley, New York, 3rd edn., 2001.
- [26] A. S. Sanz, S. Miret-Artés, Setting-up tunneling conditions by means of Bohmian mechanics, *J. Phys. A: Math. Theor.* 44 (2011) 485301(1–17).
- [27] C. Leforestier, R. H. Bisseling, C. Cerjan, M. D. Feit, R. Friesner, A. Gulberg, A. Hammerich, G. Jolicard, W. Karrlein, H.-D. Meyer, N. Lipkin, O. Roncero, R. Kosloff, A comparison of different propagation schemes for the time dependent Schrödinger equation, *J. Comp. Phys.* 94 (1991) 59–80.
- [28] D. Kosloff, R. Kosloff, A Fourier method solution for the time dependent Schrödinger equation as a tool in molecular dynamics, *J. Comp. Phys.* 52 (1983) 35–53.
- [29] R. Kosloff, D. Kosloff, A Fourier method solution for the time dependent Schrödinger equation: A study of the reaction $H^+ + H_2$, $D^+ + HD$, and $D^+ + H_2$, *J. Chem. Phys.* 79 (1983) 1823–1833.
- [30] A. S. Sanz, S. Miret-Artés, A causal look into the quantum Talbot effect, *J. Chem. Phys.* 126 (2007) 234106(1–11).
- [31] J. Egger, Volume conservation in phase space: A fresh look at numerical integration schemes, *Am. Meteor. Soc.* 124 (1996) 1955–1964.
- [32] M. Sommer, S. Reich, Phase space volume conservation under space and time discretization schemes for the shallow-water equations, *Am. Meteor. Soc.* 138 (2010) 4229–4236.
- [33] M. Shapiro, P. Brumer, *Principles of the Quantum Control of Molecular Processes*, Wiley, New York, 2003.
- [34] T. M. Coffey, R. E. Wyatt, W. C. Schieve, Monte Carlo generation of Bohmian trajectories, *J. Phys. A: Math. Theor.* 41 (2008) 335304(1–9).
- [35] S. Brandt, H. Dahmen, E. Gjonaj, T. Stroh, Quantile motion and tunneling, *Phys. Lett. A* 249 (1998) 265–270.

- [36] T. M. Coffey, R. E. Wyatt, W. C. Schieve, Quantum trajectories from kinematic considerations, *J. Phys. A: Math. Theor.* 43 (2010) 335301(1–14).
- [37] C. Fonseca-Guerra, J.-W. Handgraaf, E. J. Baerends, F. M. Bickelhaupt, Voronoi deformation density (VDD) charges: Assessment of the Mulliken, Bader, Hirshfeld, Weinhold, and VDD methods for charge analysis, *J. Comput. Chem.* 25 (2004) 189–210.
- [38] M. Born, Zur Quantenmechanik der Stoßvorgänge,, *Z. Phys.* 37 (1926) 863–867.
- [39] W. H. Zurek, J. A. Wheeler, *Quantum Theory of Measurement*, Princeton University Press, Princeton, NJ, 1983.
- [40] N. P. Landsman, Born rule and its interpretation, *Compendium of Quantum Physics: Concepts, Experiments, History and Philosophy*, Springer, Berlin, 2009.
- [41] P. Brumer, J. Gong, Born rule in quantum and classical mechanics, *Phys. Rev. A* 73 (2006) 052109(1–4).